ELSEVIER

Hearing Research 121 (1998) 11–28

HEARING RESEARCH

Spatial resolution of cochlear implants: the electrical field and excitation of auditory afferents

Andrej Kral [a,b], Rainer Hartmann [a], Dariusch Mortazavi [a], Rainer Klinke [a,*]

[a] *Physiologisches Institut III, Theodor-Stern-Kai 7, D-60590 Frankfurt/M., Germany*
[b] *Institute of Pathological Physiology, Sasinkova 4, SK-81108 Bratislava, Slovak Republic*

Received 28 May 1997; revised 26 March 1998; accepted 31 March 1998

Abstract

This paper investigates the spatial resolution of electrical intracochlear stimulation in order to enable further refinement of cochlear implants. For this purpose electrical potential distributions around a conventional human intracochlear electrode (NUCLEUS-22) were measured in a tank, in cat cadaver cochleae and in living cat cochleae. Potential gradients were calculated where of importance. The values were compared to spatial tuning curves from cat primary auditory afferents in electrical mono-, bi-, and various tripolar stimulation modes. Finally, a lumped element model was developed to elucidate the single fiber data. Tank potential measurements show the principal features of the different stimulation modes but are not sufficient to explain all the features of experimental data from single fibers. Intracochlear potential measurements indicate an increase in spatial resolution in an apical direction. The single fiber data also confirm that a tripolar stimulus configuration provides significantly better spatial resolution than any other stimulation mode presently in use.

Key words: Cochlear implant; Electrical stimulation; Auditory single fiber; Spatial resolution; Lateral inhibition

1. Introduction

Main goals in present cochlear implant research are refinement of coding strategies and improvement of spatial resolution. In patients with good preservation of the auditory nerve, the latter should lead to a restriction in the number of nerve fibers excited by one electrode channel and thus to a more natural perception.

To improve spatial resolution of electrical intracochlear stimulation the following approaches have been taken by different authors: Electrodes have been shaped as rings placed on a silastic carrier as available in the NUCLEUS-22 device (Clark et al., 1984; Patrick and Clark, 1991). Knob electrodes have been placed in a longitudinal-transversal[1] arrangement (Loeb et al., 1983) intending main currents in the direction towards the modiolus. A similar approach is taken in MedEl electrodes (Hochmair-Desoyer et al., 1983). The distance from the ganglion cells has been reduced by using a spiral array in the CLARION implant (Schindler and Kessler, 1993). For experimental purposes, the number of active electrodes in a longitudinal-transversal arrangement has been increased by techniques of laser-etching (Loeb et al., 1997).

The spatial relationship between the implant used in the present study and the primary afferent fibers (assumed to be present) is illustrated in Fig. 1. Afferent fibers which innervate inner hair cells originate from

* Corresponding author. Tel.: +49 (69) 6301 6976; Fax: +49 (69) 6301 6987; E-mail: klinke@em.uni-frankfurt.de

[1] In the present paper the term 'longitudinal' represents the basal-apical direction in the cochlea and along the axis of the tank electrode. The term 'transversal' is used in tank measurements (see Fig. 1) for measurements perpendicular to the axis of the electrode. The term transversal is further used in the cochlea for the direction from the organ of Corti to the modiolus. It thus replaces here the commonly used term 'radial'. We use the term 'radial' for currents leaving a ring electrode perpendicular to its surface. In the model, the *x*-axis corresponds to longitudinal and the *y*- and *z*-axes are summarized in the two-dimensional model to the values termed transversal in the cochlea.

0378-5955/98/$19.00
PII: S0378-5955(98)00061-6

type I ganglion cells (Spoendlin, 1988). They are myelinated up to the habenula and then lose their myelin sheath. The fibers take a transverse course from the bodies of the ganglion cells to the hair cells.

The thresholds for electrical stimulation depend on the exact orientation of the fibers concerned within the electrical field. As the type I afferents run in a transverse direction, their orientation is perpendicular to the main current component of longitudinally arranged electrode devices (Mortazavi, 1995). Orientation for electrical stimulation is therefore not optimal. Transversally oriented knob electrodes, on the other hand, would provide a more favourable field (v.d. Honert and Stypulkowski, 1987), but can only be placed with considerable effort. However, in longitudinal electrode arrays current components which flow in the transverse direction are also present. These are mainly close to the electrode rings.

Unfortunately, the exact positions of the nerve membranes which are excited by a cochlear implant are not yet known. As myelinated fibers have a lower threshold for electrical stimulation than unmyelinated ones (Ranck, 1975), it is likely that the electrical stimulus becomes effective at the habenula perforata or centrally to it.

The efficacy of a stimulus in suprathreshold activation of a neuron depends on the stimulation mode (monopolar, bipolar etc.). The thresholds for electrical stimulation by electrodes in different intracochlear positions can be determined for individual neurons. As will be shown in the present paper, electrically induced spatial tuning curves can be constructed for the neurons. The slope of these tuning curves is a measure of the spatial resolution of the stimulus. Acoustically induced tuning curves, the slopes of which are normally given in dB/octave, can be recalculated in dB/mm using a tonotopic map of the cochlea (e.g. Liberman, 1982). The electrical tuning curves can be compared to such spatial tuning curves. Note that these tuning curves are determined by a very simple criterion, namely the threshold for a defined activation of nerve fibers. A similar criterion can also be used for electrical stimulation of nerve fibers. It turns out that acoustic tuning curves are much sharper than electrically determined spatial tuning curves (Hartmann and Klinke, 1990b, see also Section 4).

To improve the sharpness of electrical tuning (spatial resolution), bipolar stimulation modes have been used instead of monopolar stimulation. There are, however, problems with bipolar stimulation: (1) Bipolar electrodes require higher currents for suprathreshold stimulation because of current shunt from electrode to electrode. (2) High potentials and high current densities form around each of the two electrodes and suprathreshold excitation is possible near both the source and the sink electrodes (Black et al., 1981).

Consequently, bipolar stimulation is not optimal. Proposals for improving spatial resolution by tripolar, quadrupolar or multipolar stimulation modes, i.e. by an introduction of 'lateral inhibitory currents' have been put forward (Ifukube and White, 1987a; Hartmann and Klinke, 1990b; Jolly et al., 1996).

The aim of this paper is to describe the determinants for spatial resolution in electrical cochlear stimulation. As current densities cannot be measured close to the excitable neurons without tissue damage, the potential fields generated by different electrode configurations were measured in a saline tank. Measurements of potential distributions were also performed in cadaver as well as in living cochleae. A lumped element model of the cochlea was elaborated to explain the results. Recordings from single auditory nerve fibers, stimulated by mono-, bi-, and various tripolar configurations were made to directly compare the differences in spatial resolution of the different stimulation modes.

2. Materials and methods

2.1. Electrical stimulation and data collection

Electrical stimulation was performed by home-made optically isolated current sources driven by sinusoids (ROCKLAND synthesizer). The potentials measured were amplified by a TEKTRONIX 5A22N differential amplifier. Signals were sampled by an AD-converter (12 bit) and stored by a MAC II computer.

2.2. Tank measurements

A human NUCLEUS-22 cochlear implant was placed in a 500-ml bath filled with Ringer's solution. The electrodes of the implant were connected to the current sources (128 Hz sinusoidal, 100 μA rms). Monopolar, monopolar vs. common ground (all other electrodes form a common indifferent electrode), bipolar and tripolar electrode configurations were tested. Tripolar configurations were used in two different modes (see Fig. 2b): without indifferent electrode, where the sum of the lateral currents equals the central current; with indifferent electrode, where part of the current flows from the central electrode to the extracochlear remote electrode, and part to the lateral electrodes. This allows variability in the lateral currents.

The potential distribution was measured with a glass-insulated Ag-electrode (tip diameter 100 μm) fixed in an ORIEL 18011 X-Y-Z positioning device (precision 1 μm) controlled by the computer. The indifferent electrode was a remote silver grid. The measurements were performed on a horizontal plane 200 μm from the implant and on a vertical plane through the central line of the horizontal plane (Fig. 1). These planes, 4×4 mm in size, were centered at the active

electrodes, measurements were performed with 100-μm steps.

To quantify the lateral spread of the potential distribution, a measure of sharpness W_{10} ('Width 10 dB', measuring the diameter of the area where the measured potential reaches or exceeds −10 dB of the maximum) was used. Similarly W_3 ('Width 3 dB') was defined for cases, where W_{10} could not be calculated because of lateral peaks. In addition, the ratio between the maximum amplitude of the potential measured above the central electrode and the maximum potential measured above the lateral electrodes was used for characterization.

2.3. Cadaver measurements

Adult cat skulls fixed in 4% formalin were used for the scala tympani measurements. The petrous bones were extirpated and the formalin was washed out with 0.1 M phosphate buffer in saline. The bulla was opened. The petrous bone was fixed in a positioning device with the round window upwards. A reference Ag electrode was fixed in the remaining section of the bulla. The round window membrane was removed with a sharp hook. One ml of Ringer's solution was very slowly introduced into the scala tympani under microscopic control. A teflon insulated gold wire (diameter 125 μm, thickness of insulation 16 μm) with an open tip was inserted into the scala tympani as deeply as possible. The impedance of the measuring electrode was 15 kΩ at 128 Hz. A NUCLEUS-22 cochlear implant was then also introduced into the scala tympani. To maintain a constant fluid level in the scala tympani, a continuous flow of Ringer's solution was provided.

A 128-Hz, 100-μA rms sinusoidal current from an optically isolated current source was fed to two neighbouring electrodes. This bipolar stimulation was chosen not to influence the values measured by the location of a remote indifferent electrode. The voltage (rms) was measured with the tip of the gold wire using a FLUKE 75 multimeter vs. the reference electrode. For further measurements, the gold wire was carefully retracted from the cochlea in 200-μm steps using a microscrew under visual control. If the NUCLEUS electrode moved the experiment was discarded. The potentials were measured at each step for each pair of active electrodes. Using this procedure, a portion of scala tympani (almost 6 mm long) could be studied.

2.4. In vivo measurements

Five adult cats were used. The animals were premedicated with 0.25 mg atropine and anaesthetized with pentobarbital (32 mg/kg i.p.), supplementary doses were given if necessary. A femoral vein was cannulated for infusion of modified Ringer's solution and supplementary doses of anaesthetic. End-tidal CO_2 was monitored and the animals were ventilated through a tracheal cannula if CO_2 exceeded 3.9%. Body temperature was maintained at 37°C with a homeothermic blanket. Both pinnae were removed and the bullae opened. The auditory nerve was exposed by a posterior fossa approach. Glass microelectrodes (impedance >20 MΩ) were inserted under visual control into the region of the internal auditory meatus for recording from primary auditory fibers (see Hartmann et al., 1984). Using acoustic stimuli, frequency tuning curves were measured. These initial recordings provided information on the position of different characteristic frequencies (CFs) within one electrode track through the auditory nerve.

When fibers with CFs between 7 kHz and 20 kHz were encountered, the ear was deafened with an intrascalar infusion of 2.5% neomycin sulphate (Upjohn). Then a NUCLEUS-22 electrode was inserted deeply into the scala tympani through the round window. In general, 11–12 rings of the human electrode could be inserted into a cat cochlea. According to Liberman (1982)'s data rings 1/2 come to lie in the 8-kHz region and rings 7/8 correspond to about 20 kHz. The thresholds of single units in the track characterized by the above described acoustic stimulation were then determined under electrical stimulation with different electrode rings. Spatial tuning curves were thus measured. The electrical stimuli consisted of sinusoids of 128 Hz or 100 μs/phase biphasic charged-balanced pulses, repetition rate 128/s. The electrode rings of the NUCLEUS-22 electrode which were not used for actual stimulation served as recording electrodes for measuring the local potential produced by the stimulus (bipolar stimulation). The indifferent electrode was placed in the temporalis muscle.

The care and use of these animals were approved by Hessian State Government.

2.5. Model

An electrical model of the cochlear duct and a NUCLEUS-22 array implanted into the scala tympani was elaborated. This model assumes a coaxial configuration of the following elements: A silastic electrode carrier, platinum electrode rings, perilymphatic fluid of the scala tympani, basilar membrane and bone, a ganglion cell and an afferent nerve fiber layer, surrounding tissue up to the remote indifferent electrode (Fig. 1). Because of the concentric configuration the 3-dimensions can be modelled by 2-dimensional lumped elements. The impedances of the different structures were represented by a resistor network (Fig. 11a) neglecting frequency dependent elements. Therefore calculations were performed with one single frequency (128 Hz) only. The x-direction (longitudinal, see Footnote 1) is represented

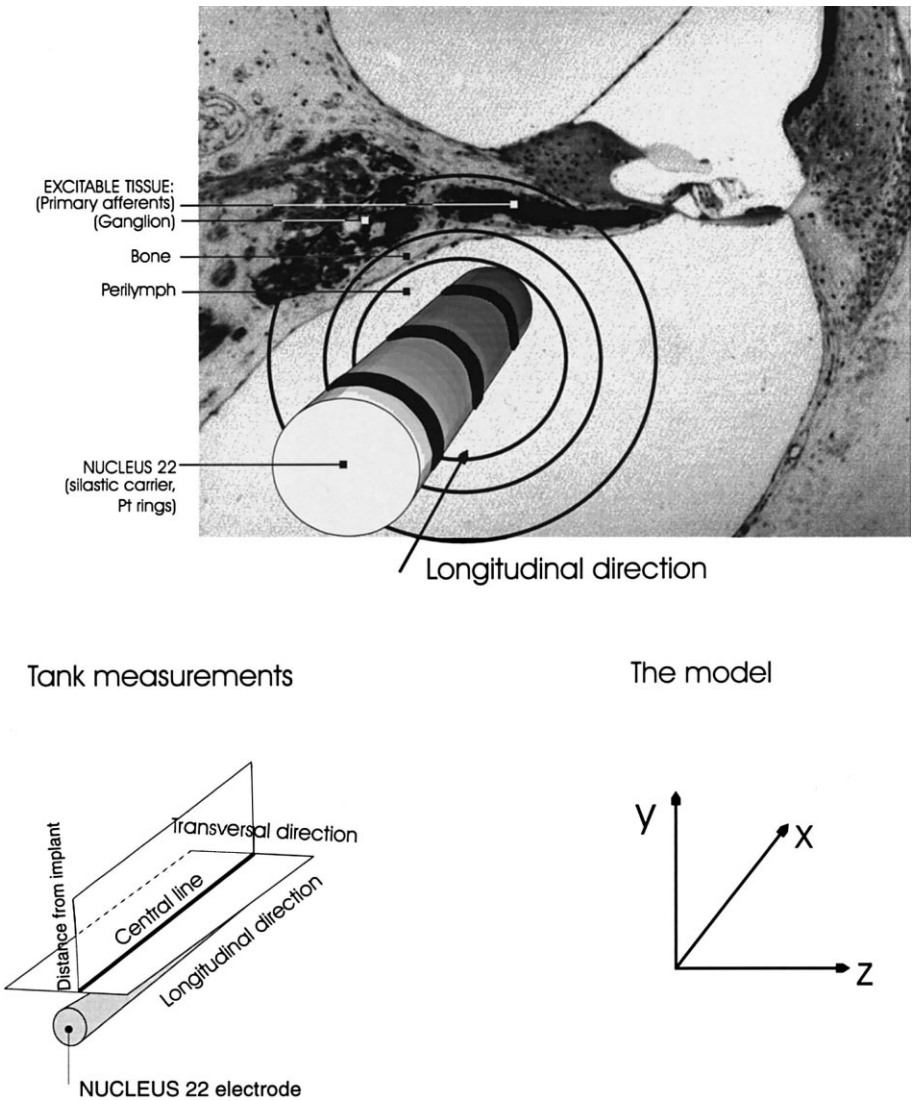

Fig. 1. Schematic illustration of an implanted cochlea. The direction from the organ of Corti to the spiral ganglion is termed 'transversal'. Below, a schematic illustration of the positions of the planes in which the potential distribution was measured in the saline tank and the definition of the axes in the cochlea model. X corresponds to longitudinal (i.e. basal to apical).

by 63 resistors r_a, 63 resistors r_c and 63 resistors r_e. The spatial resolution allows two nodes for the NUCLEUS-22 electrode spacing of 0.75 mm. The entire model covers 23.63 mm in the longitudinal direction thus exceeding the length of a NUCLEUS-22 array. The y-direction (radial) is represented by 64 resistors r_b and 64 resistors r_d (see Fig. 11a).

The different layers were represented by: silastic electrode carrier with no conductivity; the platinum rings as short-circuits; the perilymph of the scala tympani as the current shunts by the resistors $r_c(x)$ depending on the fluid space between electrode array and scala tympani wall; the pathway through the basilar membrane and the bony spiral lamina (resistors r_b); the pathway through the ganglion cells and the afferent nerve fibers in the longitudinal direction (resistors r_a); the remaining pathway to the remote indifferent electrode through the surrounding bones, muscles, etc. (resistors r_d and r_e).

The current distribution for a given input current for mono-, bi- and multipolar configurations was calculated using Kirchhoff's laws with a Borland PASCAL v. 7.0 program. The model assumes that the neural excitation occurs in either the spiral lamina (along the r_b pathway) or within Rosenthal's canal (along the r_a pathway). Whether neurons are excited depends on the strength and direction of the local electrical field close to the excitable neuronal membranes. To compare electrical threshold functions gained from single auditory nerve fibers with model threshold functions, a current trigger level for neural excitation is set by the program. This allows adjustment of the model spatial threshold curves to the single fiber thresholds measured in vivo.

3. Results

3.1. Tank measurements

Fig. 2 illustrates potentials measured in the longitudinal direction at a distance of 200 μm above the electrode array, for several electrode configurations. Values are given in mV rms. In Fig. 2a the values are normalized. The monopolar and monopolar with common ground configurations have the least sharp potential distribution. Common ground offers the advantage of a smaller W_{10} (see Table 1). In bipolar configuration the potential gradients are larger between the two active electrodes than lateral to the electrodes.

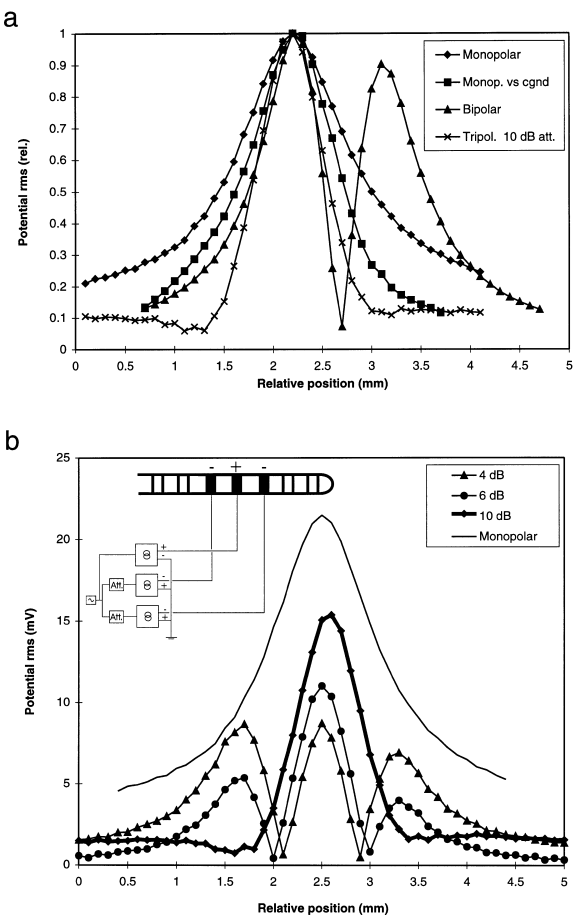

Fig. 2. a: Comparison of the potential distributions for different electrode configurations in the saline tank. The potentials are normalized to the maximum. Bipolar and tripolar −10-dB configurations show the largest potential gradients. The bipolar configuration has the disadvantage of a second peak. The stimulation was always 128 Hz 100 μA rms, distance from implant 200 μm. cgnd = common ground. b: Potential distributions for different tripolar configurations (with or without indifferent electrode) measured in the central line defined in Fig. 1. Reduction of the lateral current from −4 dB re central current to −10 dB re central current leads to an increase of the central maximum potential amplitude, the side maxima disappear. No substantial change in the potential gradients around the central peak is discernible. Stimulation always 128 Hz 100 μA rms, distance from implant 200 μm. The circuit diagram of the tripolar configuration is shown in the inset. The generator signal is fed to the electrodes via optically isolated current sources; current to the lateral electrodes can be attenuated (Att.).

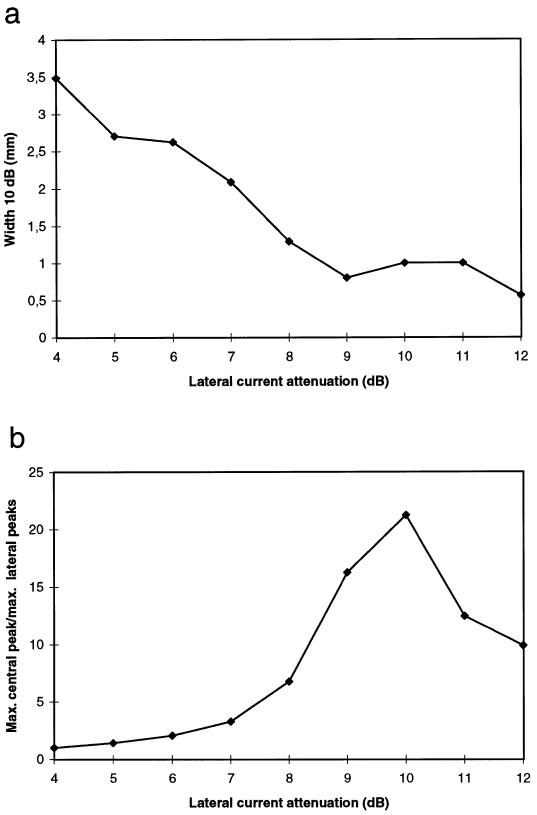

Fig. 3. a: Width 10 dB vs. attenuation of lateral currents with tripolar stimulation. A local minimum of the function is at 9 dB attenuation. Stimulation 128 Hz, 100 μA rms, distance from implant 200 μm. b: Relationship between central and lateral potential amplitudes for the tripolar configuration for different lateral currents. The maximum of the curve is at 10 dB. Stimulation 128 Hz, 100 μA rms, distance from implant 200 μm.

The results obtained with a tripolar configuration are shown in Fig. 2b. In the configuration without an indifferent electrode (6 dB attenuation of lateral currents) the central electrode acts as a source and the lateral electrodes act as sinks. Again, values were measured 200 μm above the electrode set and are given in mV rms. As can be seen, 3 maxima are formed and the lateral maxima are only 6.46 dB below the central maximum. The introduction of an additional indifferent electrode influences the lateral maxima. Fig. 2b shows that with lateral current attenuation of 4 dB the lateral potential maxima become as large as the central maximum. In this situation, the lateral currents carry more current than is sourced by the central electrode. The remote electrode becomes a source in phase with the central electrode. However, with lateral current attenuation of 6, 10 and 12 dB the lateral potential maxima are reduced so that the residual value was extremely low. Fig. 2b does not show the −12 dB case. W_{10} as a function of attenuation of lateral currents is shown in Fig. 3a. It can be seen that W_{10} shows a local minimum

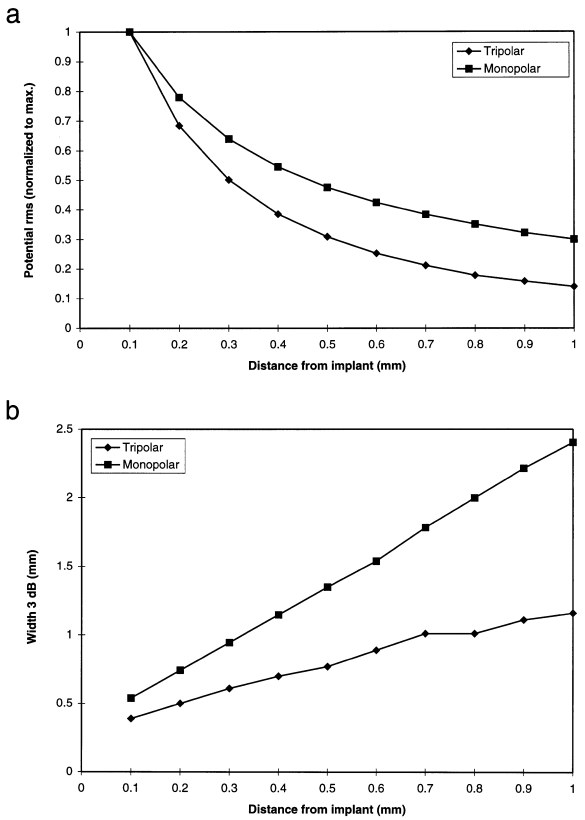

Fig. 4. Comparison of monopolar and tripolar configurations (tripolar+gnd, 10 dB lateral current attenuation) in the far field. Stimulation 128 Hz, 100 μA rms, distance from implant 200 μm. a: Changes of potential maximum amplitude with distance from the implant: comparison monopolar vs. tripolar. Bipolar data lie in between monopolar and tripolar data. b: Width 3 dB in relation to distance from the implant (radial direction, see Footnote 1) for monopolar and tripolar configurations.

at 9 dB attenuation of the lateral currents. However, if the ratio between central and lateral maxima is considered, there is an optimum at 10 dB attenuation (Fig. 3b).

The results obtained at greater distances than 200 μm are given below. The potentials measured in a plane perpendicular to the plane represented in the previous figures show an exponential decay of the maximum potential for monopolar configurations as well as for tripolar −10 dB configurations. Again the maximum amplitudes of the potentials measured in the central line are depicted for comparison (Fig. 4a). The decay of the

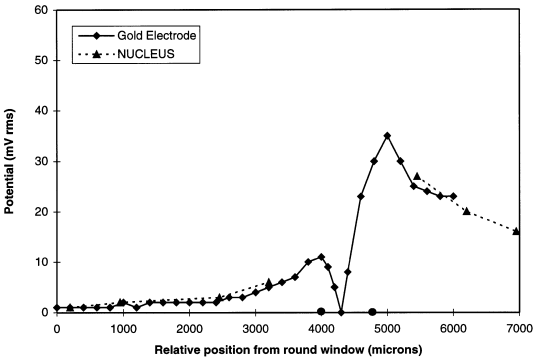

Fig. 5. Comparison of the potential distribution measured in the cadaver cochlea using the gold wire and the inactive electrode rings of the NUCLEUS-array. The good fit between the two measurements can be seen. With the NUCLEUS-array the potential at the active electrodes (full circles on the abscissa) cannot be measured. Stimulation 128 Hz, 100 μA rms, distance from implant 200 μm.

potential is steepest for the tripolar configuration. In addition, the width of the potential distribution 3 dB below maximum was measured at different distances from the implant (radial direction, Fig. 4b). It can be seen that the tripolar configuration is even more effective in sharpening the distribution of potential with increasing distance. The length constants, λ (which is defined by the equation $y = A \cdot e^{-x/\lambda}$), are 0.54 mm for monopolar and 0.43 mm for tripolar configurations, assuming an exponential decay within a distance of 0.4–1.0 mm from the active electrode.

The potential distributions measured 200 μm and 300 μm above the electrode array with monopolar configuration were used to calculate potential gradients in a radial direction (see Footnote 1). The results show that the maximum radial potential gradients are larger than the maximum longitudinal ones by a factor of 2.16. With bipolar stimulation, radial components occur mainly in the vicinity of the platinum rings. Strong longitudinal components are established between the rings (see Figs. 2 and 13). In the bipolar stimulus configurations the ratio of the maximum potential gradient in the radial vs. longitudinal direction is 0.657 determined 200 μm above the implant.

3.2. Cadaver measurements

The NUCLEUS-22 electrode set was implanted 10

Table 1
W_{10} and W_3 values for monopolar vs. bipolar and tripolar electrode configurations

	Monopolar	Monopolar cgnd	Bipolar	Tripolar −10 dB
W_{10}	3.6 mm	1.9 mm	1.3 mm 2.6 mm*	1.1 mm
W_3	0.8 mm	0.6 mm	0.4 mm 1.3 mm*	0.52 mm
Maximum	21.48 mV	18.15 mV	12.87 mV	15.07 mV

For the bipolar configuration the values for 1 single peak and both peaks (*) together are given. cgnd = common ground.

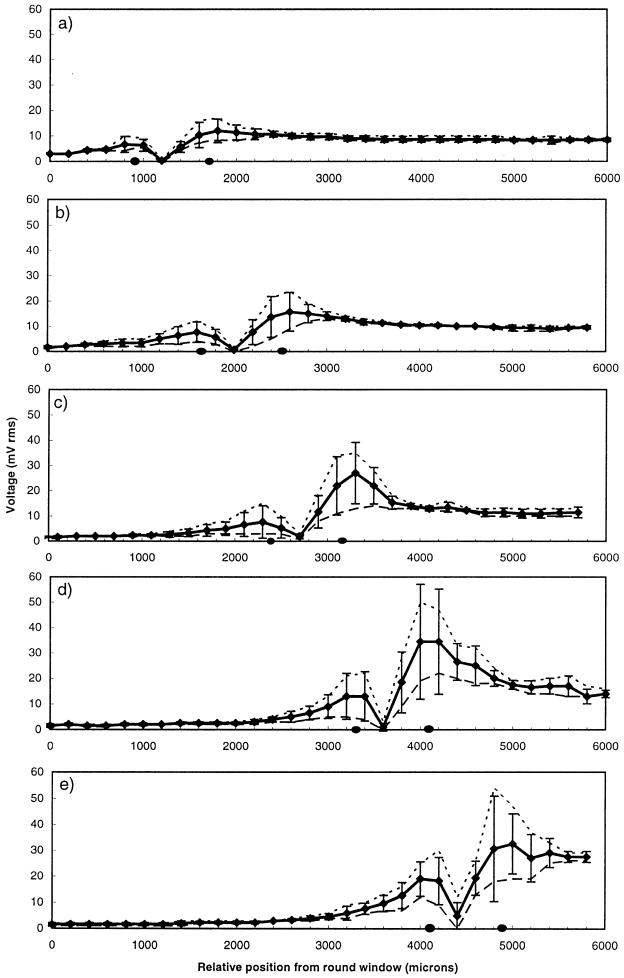

Fig. 6. Potential distributions in the cadaver cochlea for bipolar configuration with different positions of the active electrodes (full circles on the abscissa) a–e. The upper track in each panel shows the maximum potential measured at a given position for the given location of the active electrodes, middle track the mean potential with standard deviation, lower track the minimum potential measured. The peak of the potential distribution in the apical direction is always the higher one (see text). The more apically the active electrodes are located, the larger the potentials measured. Stimulation 128 Hz, 100 μA rms, distance from implant 200 μm.

times into 3 cadaver petrous bones subsequent to the placement of the gold wire. In four cases, the gold wire could be retracted smoothly so that measurements could be taken every 200 μm. To further support the data obtained with the gold wire, the inactive electrodes of the NUCLEUS implant were also used for measurements of potentials. Basically, the gold wire data agree with the NUCLEUS data. A typical result is shown in Fig. 5. The potentials are again expressed as rms-values, giving two peaks in the data obtained from the gold wire. Unfortunately active electrodes are not suitable for potential measurements.

For further evaluation the following 'normalization' was performed. The values measured were shifted along the abscissa so that the zero transitions were in register. This procedure is necessary, as electrode sets can never be introduced in exactly the same way. For each pair of active electrodes there is a specific zero transition. These zero transitions were determined for all pairs of active electrodes. For each pair of electrodes, the measured values were shifted separately longitudinally so that the zero transitions matched. This procedure results in 7 sets of data (corresponding to 7 NUCLEUS electrode pairs) separated by roughly the distance of an electrode pair. The most basal and most apical pair of active electrodes were excluded because of boundary problems so that 5 data sets remain. This procedure allows the measured data to be averaged. The results are presented in Fig. 6. The mean values and the maximum and the minimum potentials are shown. As can be seen from Fig. 6, the potentials are larger the deeper the active electrode pair is inserted (factor 3.18 between the upper and lower panels in Fig. 6). This is further illustrated in Fig. 7a, where the maximum and mean values are plotted against cochlear position. The gradient E_x of the decay of the potential in the apical direction was also calculated, whereby $E_x = \Delta\varphi/\Delta x$. The distance Δx was taken as 400 μm. Fig. 7b shows that the gradient is larger in the more apical electrode pairs. E_x changes from 1 mV/400 μm for the position 2 mm from the round window to 17 mV/400 μm determined 3 mm more apically. The corresponding W_3 values are listed in Table 2 and show that apically the W_3 values are smaller.

3.3. In vivo measurements

Attempts to use the gold wire technique in the living animal were not successful. Access to the round window is impeded by tissue and a longer gold wire is too pliable and cannot be safely introduced (the wire bends and causes bleeding in the cochlea etc). Measurements using the inactive rings of the NUCLEUS implant were therefore made and compared to those of the cadaver measurements. The potential distribution thus observed has essentially the same shape as in the cadaver measurements. Data from 6 in vivo and 4 in vitro experiments are compared in Fig. 8. Quantitatively, the in vivo measurements resulted in smaller potentials (non-significant differences; two-sided t-test at $\alpha = 5\%$) in the ap-

Table 2
W_3 values computed for maximum curves of Fig. 6

Position (μm)	W_3 (μm)
1800	874
2600	600
3400	580
4000	444
4800	500

Position column designates the position of the apical active ring in the scala tympani.

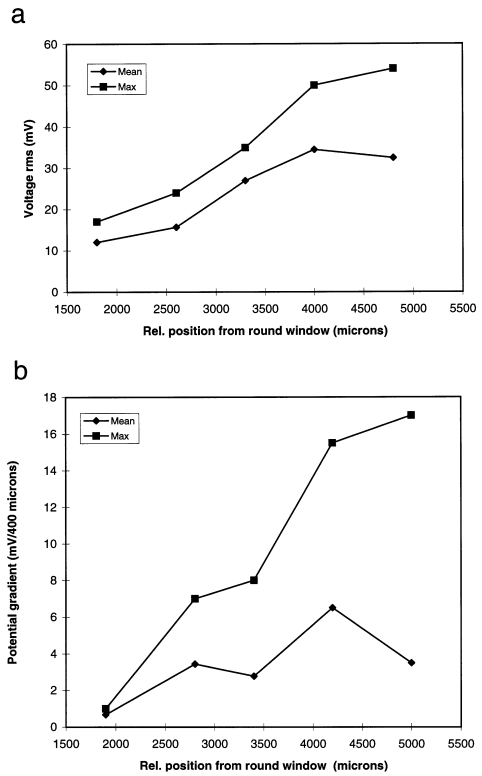

Fig. 7. a: Maximum potential (taken from maximum and mean curves of Fig. 6) in the cadaver cochlea vs. position of the corresponding active electrode. The maximum amplitude increases in the apical direction. b: Potential gradient E_x (400 μm step) measured from the maximum potential in the apical direction (for the mean and maximum curves). The gradient increases in the apical direction, particularly for the maximum curve.

ical electrodes. The potential gradient in the apical direction was 8.75 mV/750 μm in vitro and 5.88 mV/750 μm in vivo. In the basal direction the potential gradient was 3.5 mV/750 μm in vitro and 4.17 mV/750 μm in vivo. Because of differences in the spatial resolution of the gold-wire measurements and the measurements with the NUCLEUS electrode and the fact that the peak values above the active electrodes cannot be measured with the inactive rings, a direct comparison of the respective data is unfortunately not possible.

Finally, single unit thresholds with electrical stimulation in cats implanted with a NUCLEUS electrode were determined. Eighty single units were thus evaluated in

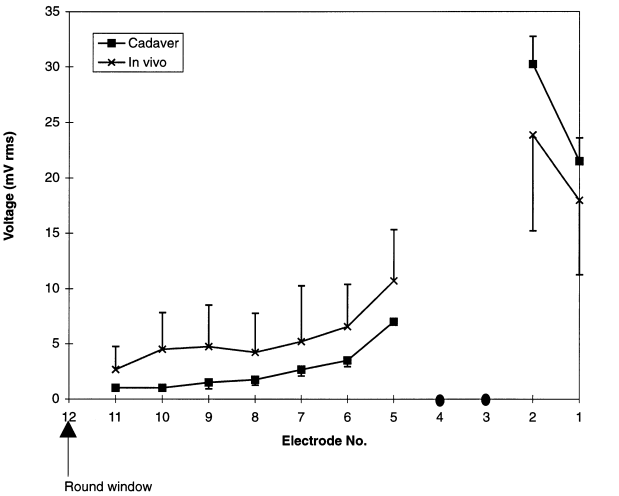

Fig. 8. Comparison of the potential distribution in the cadaver and in the living cochlea as measured by inactive electrodes of the NUCLEUS device. Electrodes 3 and 4 were active. Stimulation 128 Hz, 100 μA rms, distance from implant 200 μm. Full circles represent active electrodes.

5 cats. Fig. 9 compares examples of electrically evoked spatial tuning curves with a tuning curve determined acoustically. Normal tuning curves in the 8-kHz region are very sharp, having slopes up to 300 dB/octave (Evans, 1975), corresponding to up to 100 dB/mm recalculated for cochlear place. In comparison, the spatial tuning curves determined by electrical stimulation (sinusoids, 128 Hz) are much less sharp. In Fig. 9, electrical tuning curves are shown for monopolar, bipolar, tripolar −6-dB and tripolar −10-dB configurations. As can be seen, the lowest threshold occurs with monopolar stimulation followed by tripolar −10-dB and tripolar −6-dB stimulation. Bipolar stimulation needs the highest currents. As far as sharpness of spatial tuning is concerned tripolar −6 dB has the largest slopes, monopolar the smallest (see Table 3). The differences in slopes were significant for all configurations except for bipolar vs. tripolar −10 dB (two-sided t-test, $\alpha = 1\%$). This fact is further illustrated in Fig. 10. There examples of spatial tuning curves obtained with monopolar, bipolar, tripolar −6 dB and tripolar −10 dB are given. The neurons shown in Fig. 10 were selected for the similarity of position of their threshold minima.

Table 3
Statistics on the slopes of the spatial tuning curves calculated at the tip

	Mean slope near tip (dB/mm)	S.D. (dB/mm)	Maximum slope near tip (dB/mm)
Monopolar	3.12	2.51	10.67
Bipolar	8.47	4.49	21.33
Tripolar −6 dB	20.79	5.22	31.12
Tripolar −10 dB	9.77	3.90	16.00

The mean slope, its standard deviation and the maximal slope measured are given for each stimulation configuration.

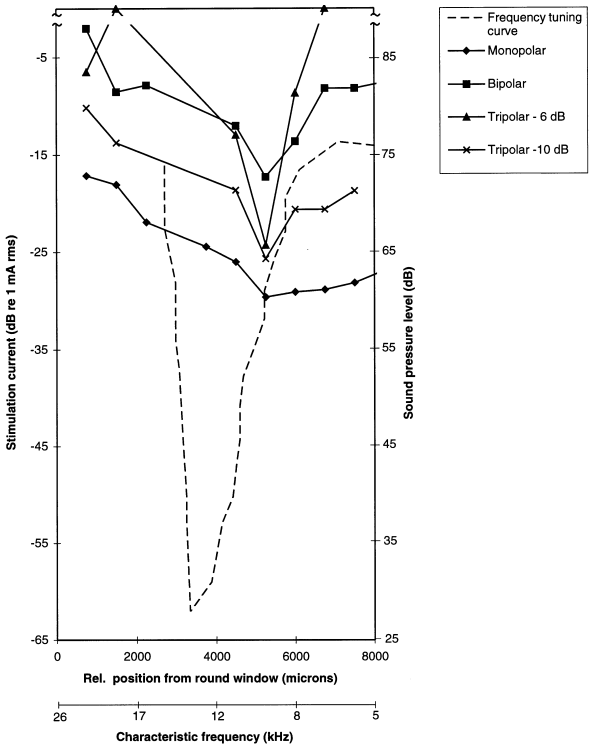

Fig. 9. Comparison of electrically evoked spatial tuning curves (monopolar, bipolar and tripolar −6 dB and −10 dB stimulation) and a sample frequency tuning curve evoked acoustically. The abscissa is given in microns from the round window. So the acoustical tuning curve is mirrored. For comparison the Liberman (1982) map is added. All electrical (spatial) tuning curves illustrated were measured in the same fiber (P109MN12). For electrodes where threshold current exceeded 1 mA rms measurements were impossible because of muscle twitches. Thus a distant (high) threshold is assumed (ordinates are broken above −5 dB).

3.4. Model

Fig. 11a gives the general concept of the network. Certain suprathreshold currents in the layers $r_b(y)$ and $r_a(x)$ were assumed to trigger action potentials. The model allows a comparison between the potentials measured in the scala tympani in vitro or in vivo and the potentials $\varphi(x)$ computed from the potential differences in the resistor layer $r_c(x)$.

The conductivities of the cochlear structures used in the model were taken from v. Bekesy (1960), Strelioff (1973), Asukuma et al. (1978), Finley et al. (1990), Suesserman (1992) and Frijns et al. (1995). The model was optimized using multiples of the resistivity of Ringer's solution with 62.25 Ω·m as follows:

$r_a(x) = 1.1$ (constant)

$r_b(y) = 10$ (constant)

$r_c(x) =$ variable

$r_d(y) = 100$ (constant)

$r_e(x) = 0.001$ (constant).

The resistors r_c are assumed to be variable because of the changing cross-sectional area of the scala tympani (A_{st}) along the cochlea (see Table 4). The A_{st} values were calculated from Hatsushika et al. (1990). Based on the results of measurements in cadaver cochleae and in vivo it was assumed that the resistor layer $r_c(x)$ is proportional to $A_1/(A_{st}(x)\text{-}A_{el})$, whereby A_1 is the cross-sectional area of the scala tympani at the apical end of the implanted electrode and A_{el} the cross-sectional area of the electrode array used. The formula applied was

$$r_c(x) = r_{c_1} \cdot \frac{A_1}{A_{st}(x) - A_{ee}}$$

whereby $r_{c_1} = 1$.

To model the cadaver implantation of 9 rings of a NUCLEUS-22 array in a cat scala tympani (Fig. 6) the longitudinal and radial current distributions for a bipo-

Table 4
Cross-sectional areas of the cat scala tympani along the cochlear duct as computed from Hatsushika et al. (1990)

Depth (μm)	Width (μm)	Height (μm)	A_{st} (mm^2)
0	3048	2362	5.654
500	3124	2438	5.982
1000	3200	2571	6.461
1500	2933	2229	5.135
2000	2895	2057	4.677
2500	2743	1867	4.022
3000	2457	1714	3.307
3500	2229	1600	2.800
4000	2000	1448	2.274
4500	1752	1295	1.782
5000	1638	1181	1.519
5500	1543	1067	1.293
6000	1448	1010	1.149
6500	1371	933	1.005
7000	1219	838	0.802
7500	1181	781	0.724
8000	1143	743	0.667
8500	1086	705	0.601
9000	1010	686	0.544
9500	952	667	0.499
10 000	952	648	0.484
10 500	914	610	0.438
11 000	838	571	0.376
11 500	781	552	0.339
12 000	781	533	0.327
12 500	762	533	0.319
13 000	762	514	0.308
13 500	762	495	0.296
14 000	724	495	0.281
14 500	724	495	0.281
15 000	724	495	0.281

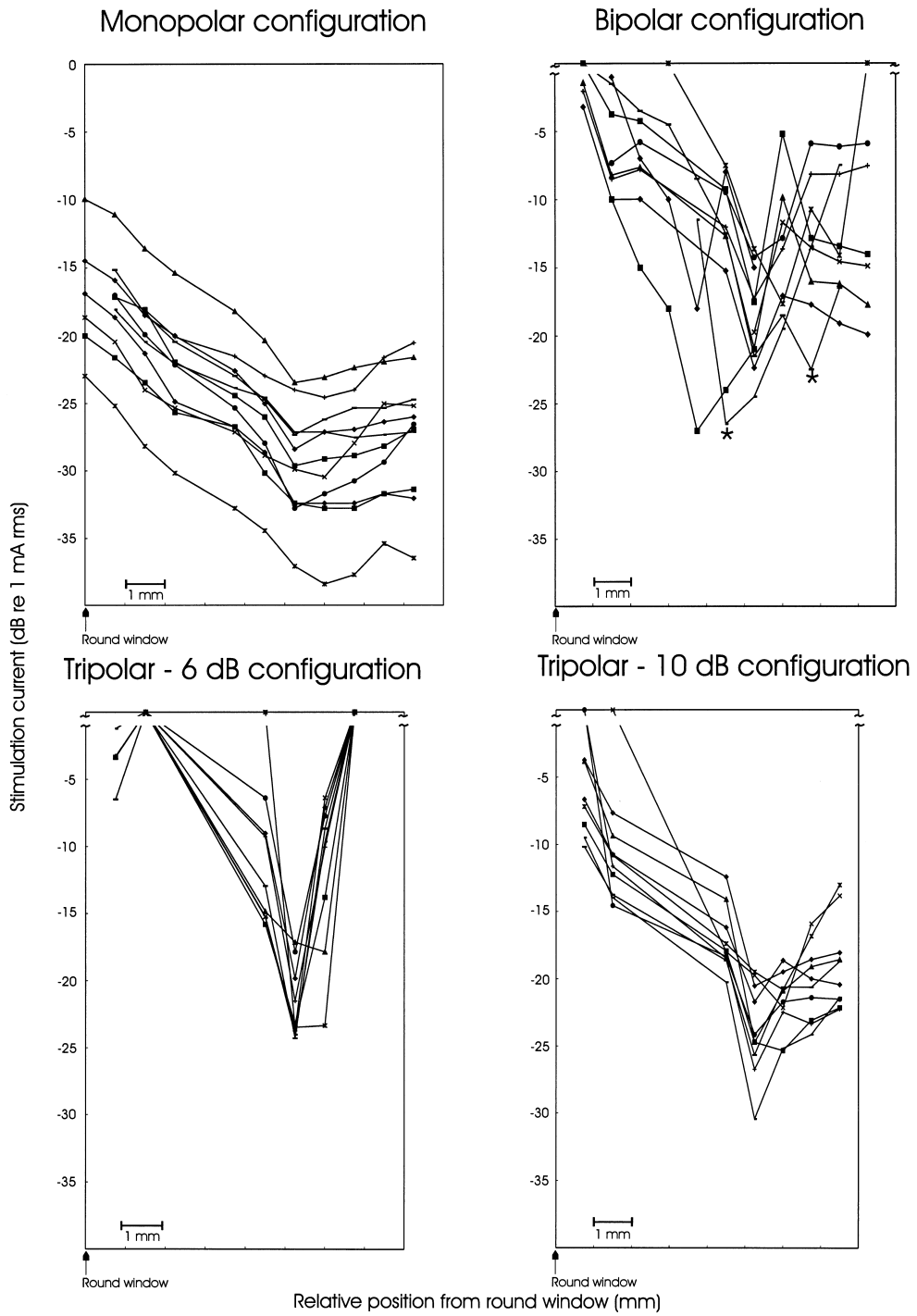

Fig. 10. Representative sample of spatial tuning curves for fibers with approximately the same position of local threshold minimum. The abscissa represents the distance from round window in the apical direction. For broken ordinate see Fig. 9. Curves marked with an asterisk were gained with charge-balanced biphasic pulses 100 μs/phase, thresholds matched to sinusoids according to identical peak-to-peak values of current.

lar stimulation with electrodes 5/6 were calculated (Fig. 11b). The current through the ganglion cell layer shows a maximum near the active electrode rings 5/6 whereas the radial current (for definition see Footnote 1) shows a negative and a positive extreme. Fig. 11c compares potentials calculated in layer c (corresponding to scala tympani) with potentials measured in the cadaver scala tympani. The decay is asymmetrical in both cases (see Section 4). The potentials are given as rms values in order to compare the results of the cadaver measurements with the model predictions. The current is given in % of the input current. (N.B.: the model gives nor-

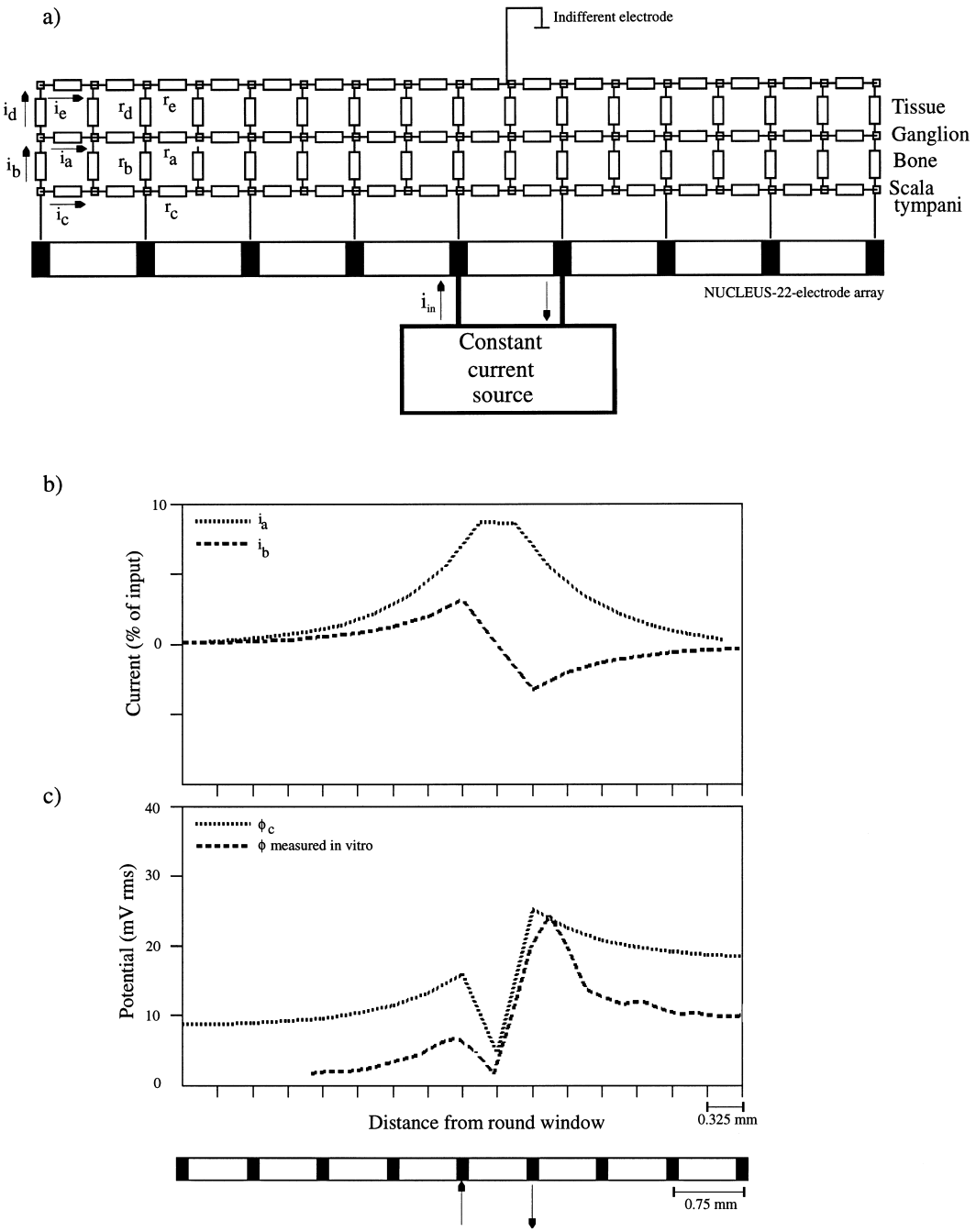

Fig. 11. a: Lumped element model of the electrical properties of the scala tympani. The model represents the resistivities of the perilymph in the scala tympani, the bone and the ganglion cell layer (r_c, r_b, r_a). The corresponding currents are termed i_c, i_b and i_a. (N.B.: the model gives normalized current values with sign.) The resistors r_d and r_e represent the surrounding tissue to allow return currents to the indifferent electrode in monopolar and tripolar −10-dB configurations. b: Longitudinal (i_a) and radial (i_b) currents in the ganglion cell layer relative to the input. The longitudinal current shows a single maximum, giving rise to 'single-tip' spatial tuning curves. The radial current shows two extremes, giving rise to tip-split spatial tuning curves. c: Comparison of the potential distribution (mV rms) in the scala tympani computed by the model and measured in the cochlea (see Fig. 6).

malized current values with sign to demonstrate not only the current amplitudes but also the direction of the current flow.)

Using the example of bipolar stimulation Fig. 12 compares electrically evoked cat spatial tuning curves with model tuning curves obtained by setting a neuronal excitation threshold. The threshold currents were set to 24 μA rms for Fig. 12a and 56 μA rms for Fig. 12b. This leads to a calculated neuronal threshold of 2 μA rms in both cases. The above model values were chosen for goodness of fit with the neuronal data illustrated. Suprathreshold longitudinal currents, i_a, fit the neuro-

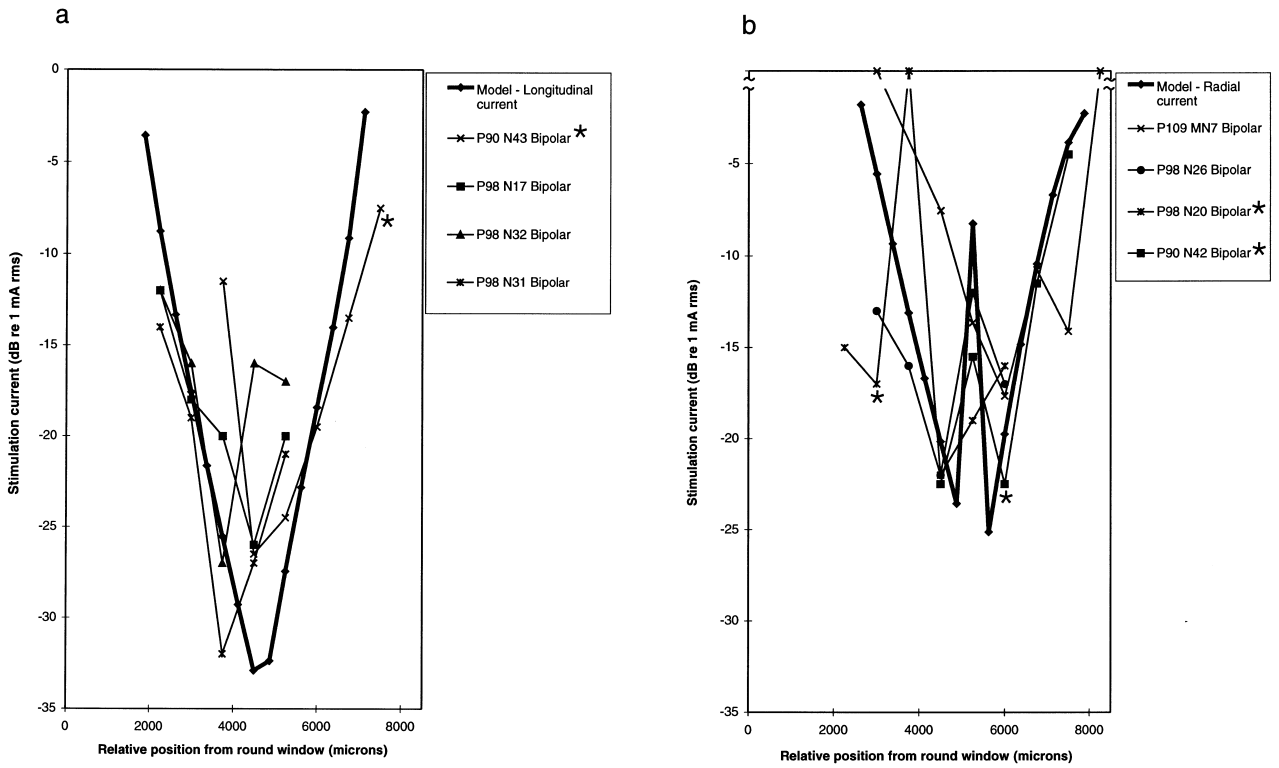

Fig. 12. a: Single unit spatial tuning curves for bipolar stimulation measured in the cat auditory nerve and model tuning curves computed according to the longitudinal current (thick line). The model shows good correspondence with animal experiments with regard to the shape and the steepness of the slopes. The threshold of the model tuning curve can be shifted arbitrarily by setting the model threshold. b: Single unit tuning curves for bipolar stimulation measured in the cat auditory nerve and model tuning curves computed according to the radial current (thick line). The model explains the tip-split tuning curves (see also a). For explanation of asterisks see Fig. 10.

nal tuning curves with one single tip (Fig. 12a). If the radial currents govern the thresholds, then threshold curves with double tips result (Fig. 12b). These are in fact seen in 31% of electrical tuning curves using bipolar stimulation. The mean depth of this notch (calculated from the higher-threshold border, i.e. the smaller values) was 5.1 dB, the maximum depth found was >17 dB. (N.B.: The entire dynamic range of a neuron stimulated electrically with sinusoids is at most 20 dB with low frequencies and decreases to as little as 3 dB with high frequencies; Hartmann et al., 1984; Hartmann and Klinke, 1990a. With pulsatile stimulation, full synchronization of action potentials is reached within 3 dB above threshold!)

The model further allows the study of longitudinal and radial currents with different electrode configurations. Monopolar as well as bipolar and tripolar configurations can be calculated. The results are presented in Fig. 13. In the monopolar case (Fig. 13a), a well defined peak is formed in the radial direction, the longitudinal currents, however, extend over a long distance. In Fig. 13b, the bipolar case is illustrated. A negative and a positive extreme are seen in the radial direction, as already mentioned in Fig. 11b. The longitudinal currents are restricted and only one positive peak can be seen. In the tripolar configuration (Fig. 13c,d), -6-dB and -10-dB cases are illustrated. In the -6-dB case, the radial peak is smaller than in the -10-dB situation, but the longitudinal currents are small and extend over a short distance only. In the -10-dB case the radial peak is larger and there are smaller lateral minima than in the -6-dB case. The longitudinal currents are, however, much larger than in the -6-dB case due to the current components flowing to the remote indifferent electrode.

4. Discussion

To date, measurements of potential distribution or electrical fields in the cochlea of humans (Black et al., 1981; Kasper et al., 1991) have been limited to a small number of measuring points for technical or ethical reasons. During cochlear implantation in humans only a few minutes of measuring time are available.

Detailed measurements with high resolution are only possible in saline tanks, in cadavers or in animal experiments. A further approach is the calculation of potential fields in electrical models of the cochlea. Different cochlear structures are represented by lumped elements out of isotropic media (Spelman et al., 1982; Finley et al., 1990; Suesserman and Spelman, 1993).

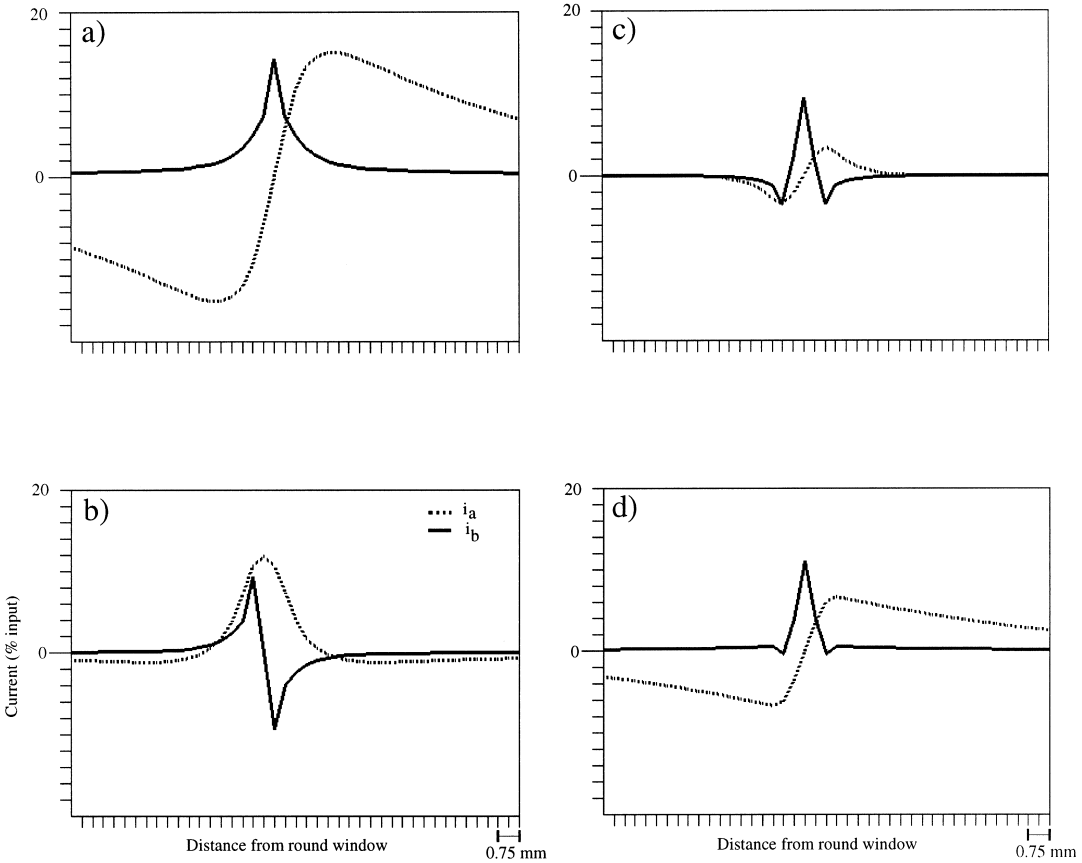

Fig. 13. a: Longitudinal (i_a, dotted line) and radial (i_b, solid line) currents in the ganglion cell layer as computed from model for monopolar configuration. The radial current is well localized, the longitudinal current shows a broad distribution and large amplitudes. Due to these large amplitudes, excitation thresholds may also be exceeded with longitudinal currents. b: Currents computed for bipolar configuration. Radial as well as longitudinal currents are well localized, but the radial current shows a positive and a negative extreme. c: Currents computed for tripolar configuration with 6-dB lateral current attenuation. Radial as well as longitudinal currents are well localized. The longitudinal current shows two extremes. d: Currents computed for tripolar configuration (10-dB lateral current attenuation, with indifferent electrode). The radial current is well localized, but the longitudinal current shows a broader distribution than in c.

4.1. Tank measurements

Tank measurements have been performed by Hochmair-Desoyer et al. (1983), Ifukube and White (1987b), Suesserman et al. (1991), Ruddy and Loeb (1995) and Jolly et al. (1996). In general, these studies were undertaken to determine the properties of the authors' own electrode systems which were developed for human or experimental use. In the present study, the properties of the most widely used human electrode, the NUCLEUS-22 electrode array, were investigated.

In considering potential distributions, it has to be kept in mind that it is not the amplitude of the potential which stimulates the neurons but the spatial gradient within the tissue. The measurement of this gradient, however, is extremely difficult as all three components in 3-dimensional space have to be determined. Nevertheless, Ifukube and White (1987b) used a double probe to measure voltage differences in a tank.

The potential distribution measured above the NUCLEUS-22 electrode in longitudinal and transversal directions allows the comparison between different stimulation modes, monopolar, bipolar and multipolar. In the case of monopolar stimulation, the potential distribution shows one single peak, which can be approximately described by a point source in an isotropic medium.

In bipolar stimulation two peaks result. The gradients of the potential function are steeper than in the monopolar case. The distance of the two peaks depends on the actual distance of the active electrodes. This has to be taken into account when stimulating patients bipolarly with greater distances (bipolar +1; bipolar +2). In principle, the current density vector close to the active electrode is directed radially under monopolar stimulation with a remote indifferent electrode. Remember, calculations from the tank measurements for monopolar configuration also show that the radial potential gradient is larger than the longitudinal one. With bipo-

lar stimulation, radial components occur mainly in the vicinity of the platinum rings. Strong longitudinal components are present between the rings.

'Lateral inhibition' (i.e. tripolar stimulation) leads to a sharpening of the potential peak (beam forming) in the longitudinal direction which in turn leads to an optimal spatial resolution of the NUCLEUS-22 electrode (see Fig. 2a). If the sharpness measure W_{10} of the different potential distributions is compared, a clear advantage of the tripolar configuration with additional indifferent electrode can be seen. The optimal value found in the tank is with lateral currents −10 dB (see Fig. 3) i.e. roughly one third of the current of the central electrode flows to both of the lateral electrodes, the resulting final current flows to the indifferent electrode. For in vivo recording of single fibers, −6 dB proves to be superior, however.

The length constant for monopolar stimulation is 1.43 mm, whereas with the tripolar −10-dB situation the length constant dropped to about half this value, i.e. 0.75 mm. The −6-dB situation in Fig. 2b corresponds to the 'quadrupolar' mode of Jolly et al. (1996). This latter configuration, however, leads to side maxima (or minima, respectively) which are only about 6 dB less than the main peak (see, however, Fig. 10 and later for discussion).

It is assumed that the tank measurements in the isotropic Ringer's solution show potential distributions as would occur in the basal region of a real human cochlea. According to Hatsushika et al. (1990), the largest diameter of the human scala tympani is about 3 mm. With an electrode diameter of 0.6 mm, a relatively large gap in the perilymphatic space is left open, certainly larger than our measuring distance in the tank of 0.2 mm. Thus potential values gained in the tank may apply for the basal scala tympani. However, the complicated structures of the cochlea are not taken into account in a tank model.

Ifukube and White (1987b) have studied the influence of bony cochlear walls on potential distribution by adding bone with and without pores to their tank and have imitated tunnel-effects by glass tubes. In fact, differences were found in this simple model. To gain a more complete insight into the situation in a cochlea (which in man narrows down from 3 mm to 0.8 mm) potentials in a real cochlea were measured and compared to neuronal data.

4.2. Cadaver measurements

In order to obtain sufficient data for the determination of the electrical field within a real cochlea a great number of measuring points are needed. However, the realization of this would damage even a cadaver cochlea to such an extent that the values measured would not be representative for an intact inner ear. The introduction of a single measuring probe in the form of an insulated gold wire and the measurement of potential values sequentially at different locations appears to be an acceptable compromise. Unfortunately, the position of the tip of the gold wire cannot be controlled with precision. Although the longitudinal position of the tip is known fairly accurately (it is retracted stepwise), the radial position is unknown and is likely to vary. It is reasonable to conclude that the highest potential values measured are the most reliable ones, as these were probably taken nearest to the platinum rings. Cochleae from cat cadavers were used for the measurements instead of human petrous bones as the cat data obtained can be easily compared with the data from electrical stimulation of primary afferent nerve fibers in living cats. The cat is particularly suitable for these measurements as the cat cochlea is embedded within the petrous bone as is a human cochlea. In guinea-pig measurements (Jolly et al., 1996) there is the risk that currents flow along different pathways, as the narrow guinea-pig cochlea stands freely in the air-filled bulla. Of course human and cat cochleae differ in dimensions. In the cat, the basal part is wider than in man, the apical parts are narrower (Hatsushika et al., 1990). Cat and human cross sectional areas are equal about 4 mm from the round window. A further source of limitation and possible error is the use of cadaver cochleae. The currents might take a quite different course in the living cochlea (see, however, Fig. 8 and later for further discussion).

The data from the basal part of the cochlea comply with the data from tank measurements. Furthermore, all data obtained with the gold wire are in agreement with measurements made with the inactive rings of the NUCLEUS-22 implant (see Fig. 5). As far as the measurements of potentials in the more apical scala tympani are concerned, the values are larger than in the tank. This is probably due to the narrower diameter of the more apical parts of the cochlear ducts. The position of the reference electrode for measurements might have influenced the offset in the potential distribution. This may influence the peak symmetry in the potential rms plots.

Simmons and Glattke (1972) and O'Leary et al. (1985) suggested that the longitudinal decay of the potentials is exponential. With this assumption, a length constant of about 0.5 mm towards the base can be calculated. However, as calculations have shown the decay does not follow an exponential pattern in the apical direction. Potential gradients also become steeper in apical regions, which is particularly clear for the maximum values illustrated in Fig. 7b. All these considerations lead to the conclusion that the spatial resolution becomes better towards the apex of the cochlea. This may be of major clinical interest as better spatial resolution of intracochlear stimuli is

important for patients. In fact, first results obtained by Gstöttner et al. (personal communication) with the introduction of intracochlear implants up to the very apex support this view. In addition the thresholds for excitation of nerve fibers should decrease in apical fibers.

4.3. In vivo studies

Measurements of ground currents in human cochlear implants (Black et al., 1981) cannot be directly compared with potential measurements. However, the paper by Kasper et al. (1991) would allow direct comparison with our data. Unfortunately, this paper is confined to monopolar stimulation with an Ineraid electrode and the graphs are on an arbitrary scale, so that no reliable calculations for comparisons can be made.

For living animals, data are available from the cat (O'Leary et al., 1985) and guinea pig (Jolly et al., 1996). The cat data have been obtained with an indirect method using a masking paradigm and combined electrical/acoustical stimulation for the estimation of length constants. The authors assume an exponential decay which generates length constants of 3–4 mm for the cat basal turn and bipolar electrical stimulation (0.75 mm distance). This is approximately a factor of 7 higher than our intracochlear data and may possibly be due to methodological differences.

Direct measurements of potential distributions in the guinea pig cochlea have been published by Jolly et al. (1996). As already argued, the free standing guinea pig cochlea may have different electrical properties than a cochlea embedded in petrous bone. Nevertheless, their data were collected with high resolution using a probe wire which was retracted in steps from the cochlea. Their data compare qualitatively well with our measurements as far as mono- and bipolar configurations are concerned. Their quadrupolar stimulation mode is identical to our tripolar −6-dB situation. Other magnitudes of lateral current using additional indifferent electrodes were not tested by these authors. Quantitative comparisons are again difficult as no quantitative data on the sharpness of potential distributions are given and the electrode distances were different (0.5 mm compared to 0.75 mm NUCLEUS-22 electrode). Also single fiber data were not provided in their paper.

The consequence of electrical fields in the living cochlea is the excitation of primary afferent nerve fibers. In humans, only a few reports on recordings of single primary afferents are available. Simmons (1966) gave a report on the electrical stimulation of afferent fibers during a surgical intervention. The patient reported auditory sensations when presented with a sinusoidal 0.5 μA_{pp} monopolar stimulus.

In contrast, a number of publications deal with the activation of single units by electrical stimulation in animals. The first reports were on units in the inferior colliculus (Merzenich and White, 1977; Black and Clark, 1980). The authors provided first data on the spatial resolution of an intracochlear electrical stimulation. These papers made use of the fact that neurons in the inferior colliculus can be driven from both ears. This feature was exploited for the estimation of resolution of intracochlear electrical stimulation. However, more direct information was available through investigators recording from primary auditory afferents (Hartmann et al., 1984; v.d. Honert and Stypulkowski, 1984; v.d. Honert and Stypulkowski, 1987; Parkins and Colombo, 1987; Hartmann and Klinke, 1990a). In the context of the present paper, only intracochlear stimulations are relevant. In these papers, thresholds for electrical stimulations were determined and used for the calculation of the spatial resolution of the electrical stimulus. The thresholds were dependent on the site of the intracochlear stimulation electrodes relative to the excited neuron. The mean slopes for spatial resolution were of the order of 3 dB/mm with monopolar sinusoidal stimulation and 7.4 dB/mm for bipolar stimulation (Hartmann and Klinke, 1990b), values considerably lower than those for the resolution of acoustic stimuli in a healthy cochlea.

Whether it is appropriate to compare acoustically and electrically generated tuning curves is open to discussion. One might argue that the dynamic range of the afferent fiber is much higher with acoustic stimuli than with electrical stimuli. The dynamic range should, however, not influence the 'threshold', i.e. the minimum stimulus necessary to activate a fiber. Determination of threshold, if the 'real' threshold can ever be found, also introduces the least error. 'Normalization' of the tuning curves based on the dynamic range of the fiber concerned would introduce new uncertainties, as the rate-intensity functions of fibers stimulated electrically develop different plateaux of activity (Hartmann et al., 1984). These plateaux depend on stimulus frequency and intensity. Such a normalization may therefore introduce a new type of artifact. We have therefore decided to compare threshold curves.

The data on slopes for spatial resolution have been extended in the present paper. The mean slope for monopolar configuration is similar in these two data-sets (3 dB/mm, Hartmann and Klinke, 1990b, vs. 3.1 dB/mm in the present paper). In bipolar stimulation the mean slopes were slightly steeper in neurons evaluated for the present paper (7.4 dB/mm vs. 8.5 dB/mm).

The present publication also provides the first single fiber data for different types of tripolar stimulation. It turns out that the tripolar −6-dB configuration produces the sharpest spatial tuning curves, with a mean slope of 20.8 dB/mm. This is 6.7 times higher than with monopolar and 2.5 times higher than with bipolar stimulation. In contrast to an initial interpretation of

the in vitro measurements, the tripolar −10-dB configuration resulted in mean slopes of 9.8 dB/mm in the spatial single fiber tuning curves. Thus, the slopes of this latter configuration are no better than the bipolar case. The tripolar −10-dB configuration appeared to be the best localized in the tank measurements. Nevertheless, in the single fiber experiment, the −6-dB configuration was shown to be superior. The apparent discrepancies can be resolved by a more detailed analysis of the results using the lumped element model. In this model, radial and longitudinal currents can be considered separately. In the tripolar −6-dB situation both radial and longitudinal currents are quite well localized, whereas the longitudinal currents are widely spread in the −10-dB case, as can be seen from Fig. 13c.

As a result of the construction of the NUCLEUS electrode, radial currents leaving the electrode surfaces will have transverse components in the cochlea (see Footnote 1 for terminology). According to the considerations on the excitability of neurons by Ranck (1975) and the actual single fiber measurements by v.d. Honert and Stypulkowski (1987), the transversally oriented currents are more effective in exciting primary afferent nerve fibers in the cochlea. Nevertheless, the longitudinal currents play an important role (as can be seen from model calculations of the poor spatial resolution of monopolar stimulation). It is most likely that the high amplitude longitudinal current causes the flat spatial tuning curves with monopolar stimulation (Fig. 13a). The tripolar −10-dB configuration may be looked upon as a combination of a monopolar and a tripolar situation, as a part of the current (4 dB) flows to the remote indifferent electrode. This may reduce the advantages of a tripolar configuration in the −10-dB case.

These considerations further indicate that measurements of potential distributions, a technique widely used by numerous authors for optimizing electrode shapes and configurations (Hochmair-Desoyer et al., 1983; Ifukube and White, 1987b; Suesserman et al., 1991; Mortazavi, 1995; Ruddy and Loeb, 1995; Jolly et al., 1996), and our own tank measurements do not provide sufficient information on spatial resolution. Potential gradients in tissue cause currents. These currents are responsible for neural excitation. According to Ranck (1975), the excitability depends on the relationship between the direction of myelinated nerve fibers and the stimulation current. Currents perpendicular to the nerve fiber are less effective than currents parallel to the fibers. Currents therefore need to be considered in relation to their paths. This factor is included in our model. Of course the excitability of the fibers may also depend on current in a more complex way (e.g. activation function, Rattay, 1989). However, it appears to be the longitudinal current component, that is responsible for the differences between the tank measurements and the single unit recordings.

Another interesting result is the tip splitting observed in electrically evoked spatial tuning curves. With bipolar stimulation the spatial tuning curves frequently display two minima with a central maximum in between. The differences between this maximum and the two adjacent minima is of the order of 5 dB. This does not appear significant. However, this value must be considered within the context of the whole dynamic range of an electrically stimulated afferent fiber. This dynamic range depends on stimulation pattern. It is 20 dB at most with sinusoids of low frequencies and decreases to as low as 3 dB with high frequencies or pulsatile stimuli (Hartmann et al., 1984, Hartmann and Klinke, 1990a). The mean differences between the two tips and the intercalated maximum is therefore of the order of the neuron's dynamic range!

This tip splitting can be observed in 31% of fibers stimulated with bipolar electrodes. It is apparently the fine geometry of the location of the fiber relative to the position of the stimulating electrodes that is responsible for the structure of the spatial tuning curve. If the fiber runs exactly between the two electrode rings, the radial current (i_b in Fig. 13b) will be zero. In this case, the neuron can only be activated by the longitudinal current i_a and tip splitting in the spatial tuning curve does not arise. If, however, the fiber is located closer to one of the electrode rings, both radial and longitudinal currents may contribute to the excitation of the fiber and tip splitting may result.

Whatever the exact reason for tip splitting may be, it does occur in a large proportion of afferent fibers when stimulated bipolarly. It is possible that this feature also contributes to the artificial character of the perceptions evoked by cochlear implants.

4.4. Model

Although the model presented here is a simplification it does provide an explanation of the single fiber data. In a real cochlea, currents will take various paths because of the different impedances of the tissues concerned. More elaborate models exist (e.g. Frijns et al., 1995), but the present model is merely intended to represent currents which can be expected near the excitable membranes. The model provides a close fit with our experimental condition. As the calculations are performed using one single stimulation frequency, the neglect of capacitances also appears to be acceptable. The non-zero asymptote of the potentials (Fig. 11c) is a boundary effect caused by the finite length of the chain.

Limitations of the present model are: It does not allow the investigation of time-frequency effects and it is only intended to clarify spatial resolution. It is limited

to two dimensions and ignores the spiral configuration of the cochlea. It simplifies the structure of the scala tympani in assuming a straight tube. It is assumed that the excitability of neurons in layers close to the electrodes is represented properly. With strong currents, the spiral shape of the cochlea might lead to activation of remote structures (e.g. in the modiolus), a feature that cannot be shown by the model.

5. Conclusions

Although the present data were obtained with a NUCLEUS electrode array, the results are assumed to be qualitatively applicable to other electrode systems. The following may be postulated: (a) The introduction of a tripolar −6-dB configuration should substantially improve the spatial resolution of cochlear implants. (b) From the increase of potentials and improvement of spatial resolution in the cadaver measurements and from model calculations, it can be concluded that filling up the scala tympani with electrically insulating material may prevent current shunts and thus also improve thresholds and spatial resolution. (c) Introducing electrode arrays up to the helicotrema would not only stimulate apical fibers but also serve to improve of spatial resolution in humans and restore natural cochleotopic representation.

Acknowledgments

This work was supported by the Deutsche Forschungsgemeinschaft (SFB 269). A.K. was a recipient of a grant by the DAAD. We thank the NUCLEUS-COCHLEAR company Europe, Basle, for the donation of NUCLEUS-22 arrays. We also thank Thomas Wulf and Karl F. Winter for excellent technical equipment. Ms. Silvia Heid is thanked for Fig. 1. The authors finally wish to thank the anonymous referees for their critical comments on an earlier version of this paper, which stimulated further experiments.

References

Asukuma, S., Snow, J.B., Jr., Murakami, Y., 1978. Electrical resistance of the cochlear partition. Hear. Res. 1, 25–30.

v. Bekesy, G., 1960. Experiments in Hearing. McGraw-Hill, New York.

Black, R.C., Clark, G.M., Patrick, J.F., 1981. Current distribution measurement within the human cochlea. IEEE Trans. Biomed. Eng. 28, 721–724.

Black, R.C., Clark, G.M., 1980. Differential electrical excitation of the auditory nerve. J. Acoust. Soc. Am. 67, 868–874.

Clark, G.M., Tong, Y.C., Patrick, J.F., Seligman, P.M., Crosby, P.A., Kuzma, A.J., Money, D.K., 1984. A multichannel hearing prosthesis for profound-to-total hearing loss. J. Med. Eng. Tech. 8, 3–8.

Evans, E.F., 1975. Cochlear nerve and cochlear nucleus. In: Keidel, W.D., Neff, W.D. (Eds.), Handbook of Sensory Physiology, Vol. 5/2. Springer, New York, 1–108.

Finley, C.C., Wilson, B.S., White, M.W., 1990. Models of neural responsiveness to electrical stimulation. In: Miller, J.M., Spelman, F.A. (Eds.), Cochlear Implants: Models of the Electrically Stimulated Ear. Springer, New York, 55–96.

Frijns, J.H.M., de Snoo, S.L., Schoonhoven, R., 1995. Potential distributions and neural excitation patterns in a rotationally symmetric model of the electrically stimulated cochlea. Hear. Res. 87, 170–186.

Hartmann, R., Klinke, R., 1990a. Response characteristics of nerve fibres to patterned electrical stimulation. In: Miller, J.M., Spelman, F.A. (Eds.), Cochlear Implants. Models of the Electrically Stimulated Ear. Springer Verlag, New York, 135–160.

Hartmann, R., Klinke, R., 1990b. Impulse patterns of auditory nerve fibres to extra and intracochlear electrical stimulation. Acta Otolaryngol. (Suppl.) 469, 128–134.

Hartmann, R., Topp, G., Klinke, R., 1984. Discharge patterns of cat auditory nerve fibres with electrical stimulation of the cochlea. Hear. Res. 13, 47–62.

Hatsushika, S., Shepherd, R.K., Clark, G.M., Tong, I.C., Funasaka, S., 1990. Dimensions of the scala tympani in the human and cat with reference to cochlear implants. Ann. Otol. Rhinol. Laryngol. 99, 871–876.

Hochmair-Desoyer, I.J., Hochmaier, E.S., Burian, K., 1983. Design and fabrication of multiwire scala tympani electrodes. In: Parkins, C.W., Anderson, S.W. (Eds.), Cochlear Prostheses. Annals of the New York Academy of Sciences 405, 173–182.

v.d. Honert, C., Stypulkowski, P.H., 1984. Physiological properties of the electrically stimulated auditory nerve. II. Single fiber recordings. Hear. Res. 14, 225–244.

v.d. Honert, C., Stypulkowski, P.H., 1987. Single fiber mapping of spatial excitation patterns in the electrically stimulated auditory nerve. Hear. Res. 29, 195–206.

Ifukube, T., White, L., 1987a. A speech processor with lateral inhibition for an eight channel cochlear implant and its evaluation. IEEE Trans. Biomed. Eng. 34, 876–882.

Ifukube, T., White, L., 1987b. Current distributions produced inside and outside the cochlea from scala tympani electrode array. IEEE Trans. Biomed. Eng. 34, 883–890.

Jolly, C.N., Spelman, F.A., Clopton, B.M., 1996. Quadrupolar stimulation for cochlear prostheses: Modelling and experimental data. IEEE Trans. Biomed. Eng. 43, 857–865.

Kasper, A., Pelizzone, M., Montandon, P., 1991. Intracochlear potential distribution with intracochlear and extracochlear electrical stimulation in humans. Ann. Otol. Rhinol. Laryngol. 100, 812–816.

Liberman, M.C., 1982. The cochlear frequency map for the cat: Labeling auditory nerve fibers of known characteristic frequencies. J. Acoust. Soc. Am. 72, 1441–1449.

Loeb, G.E., Byers, C.L., Rebscher, S.J., Casey, D.E., Fong, M.M., Schindler, R.A., Gray, R.F., Merzenich, M.M., 1983. Design and fabrication of an experimental cochlear prosthesis. Med. Biol. Eng. Comput. 21, 241–254.

Loeb, G.E., Peck, R.A., Rubinstein, J.T., Rebscher S.J., 1997. A highly selective cochlear electrode array. Conference on implantable auditory prostheses, Pacific Grove, CA, Abstracts p. 89.

Merzenich, M.M., White, M.W., 1977. Cochlear implant. The interface problem. In: Hambrecht, F.T., Reswick, J.B. (Eds.), Biomedical Engineering and Instrumentation: Functional Electrical Stimulation 3. Dekker, New York, NY, pp. 321–340.

Mortazavi, D., 1995. Untersuchungen zur Einschränkung des Elektrischen Feldes und Verbesserung der Kanaltrennung bei Intracochleärer Elektrischer Reizung. Thesis, J.W. Goethe-Universität, Frankfurt am Main, Germany.

O'Leary, S.J., Black, R.C., Clark, G.M., 1985. Current distributions in the cat cochlea: A modelling and electrophysiological study. Hear. Res. 18, 273–281.

Parkins, C.W., Colombo, J., 1987. Auditory-nerve single-neuron thresholds to electrical stimulation from scala tympani electrodes. Hear. Res. 31, 267–286.

Patrick, J.F., Clark, G.M., 1991. The Nucleus 22-channel cochlear implant system. Ear Hear. 12, Suppl., 3S–9S.

Ranck, J.B., 1975. Which elements are excited by electrical stimulation of mammalian central nervous system: a review. Brain Res. 98, 417–440.

Rattay, F., 1989. Analysis of models for extracellular fiber stimulation. IEEE Trans. Biomed. Eng. 36 (7), 676–682.

Ruddy, H.A., Loeb, G.E., 1995. Influence of materials and geometry on fields produced by cochlear electrode arrays. Med. Biol. Eng. Comput. 33, 793–801.

Schindler, R.A., Kessler, D.K., 1993. Clarion cochlear implant: phase I investigation results. Am. J. Otol. 14, 263–272.

Simmons, F.B., 1966. Electrical stimulation of the auditory nerve in man. Arch. Otolaryngol. 84, 2–54.

Simmons, F.B., Glattke, T.J., 1972. Comparison of electrical and acoustical stimulation of the cat ear. Ann. Otol. Rhinol. Laryngol. 81, 731–738.

Spelman, F.A., Clopton, B.M., Pfingst, B.E., 1982. Tissue impedance and current flow in the implanted ear; implications for the cochlear prosthesis. Ann. Otol. Rhinol. Laryngol. 91 (Suppl. 98), 1–8.

Spoendlin, H., 1988. Neural anatomy of the inner ear. In: Jahn, A.F., Santos-Sacchi, J. (Eds.), Physiology of the Ear. Raven Press, New York, 201–219.

Strelioff, D., 1973. A computer simulation of the generation and distribution of cochlear potentials. J. Acoust. Soc. Am. 54, 620–629.

Suesserman, M.F., 1992. Noninvasive Microelectrode Measurement Technique for Performing Quantitative, in vivo Measurements of Inner Ear Impedances. PhD Thesis, University of Washington.

Suesserman, M.F., Spelman, F.A., Rubinstein, J.T., 1991. In vitro measurement and characterization of current density profiles produced by nonrecessed, simple recessed and radially varying recessed stimulating electrodes. IEEE Trans. Biomed. Eng. 38, 401–408.

Suesserman, M.F., Spelman, F.A., 1993. Lumped-parameter model for in vivo cochlear stimulation. IEEE Trans. Biomed. Eng. 40, 237–245.